

Atmospheric Electron Spectrum above 30 GeV at the high altitude

Y. Komori^a, T. Kobayashi^b, K. Yoshida^c, J. Nishimura^d

^a*Kanagawa University of Human Services, Yokosuka 238-8522, Japan,
komori-y@kuhs.ac.jp, 81-46-828-2759*

^b*Department of Physics, Aoyama Gakuin University, Sagamihara 229-8558, Japan*

^c*College of Systems Engineering and Science, Shibaura Institute of Technology, Saitama
337-8570, Japan*

^d*The Institute of Space and Astronautical Science, JAXA, Sagamihara 229-8510, Japan*

Abstract

We have observed the primary electron spectrum from 30 GeV to 3 TeV using emulsion chambers flown by balloons at the top of the atmosphere, for the purpose of exploring the origin of cosmic rays in the Galaxy. The atmospheric gamma rays have been simultaneously observed in the 30 GeV \sim 8 TeV energy range. In this paper, we estimate the atmospheric electron spectrum in the upper atmosphere (< 10 g/cm²) from our observed gamma-ray spectrum using the electromagnetic shower theory in order to derive the primary cosmic-ray electron spectrum. The transport equations of the electron and gamma-ray spectrum are analytically solved and the results are compared with those of Monte Carlo simulation (MC). Since we used the observed atmospheric gamma rays as the source of atmospheric electrons, our solutions are free from ambiguities on the primary cosmic-ray nuclear spectra and nuclear interaction models included in MC. In the energy range above several hundred GeV, the Dalitz electrons produced directly from neutral pions contribute around 10 percent to the whole atmospheric electron spectrum at the depth of 4 g/cm², which increases in importance at the higher altitude and cannot be ignored in TeV electron balloon observations.

Keywords: cosmic-ray electrons, atmospheric electrons, shower theory, nuclear interaction models

1. Introduction

The primary electrons above 30 GeV using balloon-borne emulsion chambers have been observed since 1960's [1][2][3]. The major purpose of primary electron observations is to investigate the transport and the origin of cosmic rays in the Galaxy, and so far one believes that the most likely sources of electrons are supernova remnants such as Vela SNR [2]. High-energy cosmic-ray electrons rapidly lose their energy because of the synchrotron radiation in the Galactic magnetic field and inverse-Compton scattering with the Galactic photons. These processes cause a steeper spectrum with the index of $-(3.0 \sim 3.3)$. On the other hand, cosmic-ray protons have the spectral index of around -2.7 . Therefore the atmospheric electrons increase the ratio to primary electrons because they have the same spectral index as the protons. In order to derive the primary electron spectrum in balloon experiments, it is required to subtract the atmospheric electron spectrum produced in residual atmosphere.

Atmospheric electrons above 10 GeV are mostly due to the pair productions of gamma rays produced in the hadronic interactions in the residual atmosphere. Those gamma rays are mainly due to the decays of π^0 mesons with smaller fractions from η mesons, K mesons, etc. In this paper we estimate the atmospheric electron spectrum from the observed gamma-ray spectrum and show the contribution of the Dalitz electrons which are directly produced electrons from π^0 and η mesons, that is not through gamma rays. In addition, we consider the direct production of electrons from K and π^\pm mesons, which contributes in the lower energy range below 100 GeV and increases with decreasing energy. The first precise estimates of atmospheric electron flux was calculated by Orth & Buffington [4]. They have given the atmospheric electrons in the 1-100 GeV energy range contributed from the decay of mesons produced by nuclear interactions. Their calculations are based on MC techniques and they presented just a simple analytic model which summarize their MC results. On the other hand, we estimate the flux of atmospheric electrons from the observed gamma rays by using the electromagnetic shower theory. The results are compared to the MC results assuming the primary hadron flux and nuclear interaction model, and discuss the behavior of both electron and gamma-ray spectra in the upper atmosphere.

2. Calculations

We consider the transport equations of the electron and gamma-ray spectrum above 10 GeV in the atmosphere ($< 10\text{g/cm}^2$) based on the electromagnetic shower theory of Approximation A [5] which treats the behavior of electromagnetic interaction in the upper atmosphere. The atmospheric electrons are mostly produced by gamma rays, originated from π^0 decay mode, η and K^0 decay mode, etc. The equation should include the production rate of atmospheric gamma rays from those mesons. We estimate the production rate from the atmospheric gamma-ray spectrum $J_\gamma(E)$ observed simultaneously in our primary electron experiments [6]:

$$J_\gamma(E)(\text{m}^2 \cdot \text{s} \cdot \text{sr} \cdot \text{GeV})^{-1} = (1.12 \pm 0.13) \times 10^{-4} (E/100\text{GeV})^{-2.73 \pm 0.06}, \quad (1)$$

in the range from 30 GeV to 8 TeV, which is the vertical gamma-ray spectrum normalized at 4.0 g/cm^2 originating from hadronic interactions of primary protons and heavy nuclei with the residual atmosphere. The contribution from primary electrons is subtracted.

2.1. Formulation and Solution

At the depth t in the atmosphere, the number of electrons, $\pi(E, t)dE$, and gamma-rays, $\gamma(E, t)dE$, with energies between E and $E + dE$ satisfy the following simultaneous equations.

$$\frac{\partial \pi(E, t)}{\partial t} = -A'\pi(E, t) + B'\gamma(E, t) + \pi_D(E, t) \quad (2)$$

$$\frac{\partial \gamma(E, t)}{\partial t} = C'\pi(E, t) - \sigma_0\gamma(E, t) + \gamma_{ex}(E, t) \quad (3)$$

As shown in the literature [5], the operator A' represents the effect of the radiation loss process, B' the pair production, C' the gamma ray contributed from electrons, and σ_0 the absorption by the pair production. The functional forms of these operators are shown in Appendix A.

In eq. (3), we add the gamma-ray production rate from nuclear interactions as:

$$\gamma_{ex}(E, t)dE = k_g E^{-\beta-1} \exp(-t/L)dE, \quad (4)$$

in which the spectral index $\beta = 1.73$ is determined from eq. (1). The attenuation path length is assumed as $L = 100 \text{ g/cm}^2$ [6], giving the uncertainty of a

few percent to the production rate at the depth of 10 g/cm². The coefficient k_g is estimated from the observed gamma ray spectrum of eq. (1). Gamma rays are mostly produced through the π^0 decay mode and other small contributions exist from the η and K^0 decay mode, which give the fraction of 0.16 and 0.03, respectively, to the π^0 decay mode for the spectral index of around 1.7 [6].

In the eq. (2) we include the small contribution of electrons from the nuclear interaction of Dalitz decay mode, which is the second major mode of π^0 decay, producing one real gamma ray and one electron-positron pair, occupying 1.2% of π^0 decay process [7]. The production rate of Dalitz electron pairs is estimated as a fraction of the gamma ray production rate as follows:

$$\pi_D(E, t) = a \cdot \gamma_{ex}(E, t) . \quad (5)$$

The coefficient a is estimated from the decay rate of Dalitz electrons from the π^0 and η mesons, and the result is given by $a = 4.9 \times 10^{-3}$ (see Appendix B).

The initial condition of electron spectrum at the top of the atmosphere is the primary electron spectrum [1] and that of the gamma-ray spectrum is the Galactic diffuse gamma rays, which is assumed to be zero. We have

$$\begin{aligned} \pi(E, 0) &= 1.6 \times 10^{-4} \left(\frac{E}{100 \text{ GeV}} \right)^{-3.3} \\ &\quad (\text{m}^2 \cdot \text{sr} \cdot \text{sec} \cdot \text{GeV})^{-1} , \\ \gamma(E, 0) &= 0 . \end{aligned} \quad (6)$$

The eq. (6) gives the electron spectral index of $\alpha = 2.3$.

The transport equations are solved using the above conditions. The solution of electron spectrum at the depth t becomes

$$\pi(E, t) = \pi(E, 0)\zeta(t) + \gamma_{ex}(E, t)\xi(t) , \quad (7)$$

$$\begin{aligned} \zeta(t) &= \frac{[(\lambda_1 + \sigma_0)e^{\lambda_1 t} - (\lambda_2 + \sigma_0)e^{\lambda_2 t}]}{\lambda_1 - \lambda_2} , \\ \xi(t) &= \frac{B(\beta)}{\lambda_1 - \lambda_2} \left[\frac{e^{(\lambda_1 + \frac{1}{L})t} - 1}{\lambda_1 + 1/L} - \frac{e^{(\lambda_2 + \frac{1}{L})t} - 1}{\lambda_2 + 1/L} \right] \\ &\quad + \frac{a}{\lambda_1 - \lambda_2} \times \\ &\quad \left[\frac{(\lambda_1 + \sigma_0)e^{(\lambda_1 + 1/L)t} - (\sigma_0 - 1/L)}{\lambda_1 + 1/L} \right] \end{aligned}$$

$$-\frac{(\lambda_2 + \sigma_0)e^{(\lambda_2+1/L)t} - (\sigma_0 - 1/L)}{\lambda_2 + 1/L} \Big] .$$

The coefficient $\zeta(t)$ represents the energy loss rate of electrons by bremsstrahlung in the atmosphere. The term $\gamma_{ex}(E, t)\xi(t)$ represents the atmospheric electron spectrum. The first term of $\xi(t)$ represents the pair production rate from gamma rays and the second term including a is the contribution from Dalitz decay mode. The atmospheric gamma-ray spectrum at the depth t g/cm² is given by

$$\gamma(E, t) = \pi(E, 0)\eta_1(t) + \gamma_{ex}(E, t)\eta_2(t) , \quad (8)$$

$$\eta_1(t) = \frac{C(\alpha)}{\lambda_1 - \lambda_2} [e^{\lambda_1 t} - e^{\lambda_2 t}] ,$$

$$\eta_2(t) = \frac{1}{\lambda_1 - \lambda_2} [f(\lambda_1) - f(\lambda_2)] ,$$

$$f(\lambda) = \frac{1}{\lambda + 1/L} \{ (\lambda + A(\beta))e^{(\lambda+1/L)t} - (A(\beta) - \frac{1}{L}) + a \cdot C(\beta)(e^{(\lambda+1/L)t} - 1) \} ,$$

where η_1 represents the gamma-ray production rate from primary electrons and η_2 represents the attenuation rate of gamma rays by pair production. The coefficient $\lambda_1(s)$, $\lambda_2(s)$, $A(s)$, $B(s)$, $C(s)$ and σ_0 with $s = \alpha, \beta$ used above equations are well known formulas and given in Appendix A.

The approximate expression of atmospheric electron spectrum becomes

$$\xi(t) \cdot \gamma_{ex}(E, t) \sim \left(\frac{B(\beta)}{2} t^2 + a \cdot t \right) \gamma_{ex}(E, t) ,$$

which corresponds to the estimate of atmospheric electron spectrum in the Orth&Buffington's paper [4].

The production rate of gamma rays eq. (4) estimated from the eq. (8) and the eq. (1) is given by

$$\gamma_{ex}(E, t) = 1.11 \times 10^{-3} (E/100 \text{ GeV})^{-2.73} \exp\left(\frac{-t}{100 \text{ g/cm}^2}\right) (\text{m}^2 \cdot \text{s} \cdot \text{sr} \cdot \text{GeV} \cdot \text{r.l.})^{-1} ,$$

in which the radiation length of air is taken as 36.6 g/cm² [7].

2.2. Solution with Zenith Angle Distribution

As cosmic rays come in all directions, the intensities in the previous section should be integrated with the acceptance angle θ of each detector. At the depth t , the electron differential spectrum $j_{ob}(E, t)$ and the gamma-ray spectrum $\gamma_{ob}(E, t)$ are derived as follows.

$$\begin{aligned}
j_{ob}(E, \theta, t) & (\text{m}^2 \cdot \text{sec} \cdot \text{GeV}^{-1}) \\
&= 2\pi \int_0^\theta \pi(E, \frac{t}{\cos \theta}) \cos \theta \sin \theta d\theta \\
&= \pi(E, 0)\zeta(\alpha, \theta, t) + \gamma_{ex}(E, t)\xi(\beta, \theta, t)
\end{aligned} \tag{9}$$

$$\begin{aligned}
\gamma_{ob}(E, \theta, t) & (\text{m}^2 \cdot \text{sec} \cdot \text{GeV}^{-1}) \\
&= 2\pi \int_0^\theta \gamma(E, \frac{t}{\cos \theta}) \cos \theta \sin \theta d\theta \\
&= \pi(E, 0)\eta_1(\alpha, \theta, t) + \gamma_{ex}(E, t)\eta_2(\beta, \theta, t)
\end{aligned}$$

The coefficients of each term are calculated from the following expressions,

$$\begin{aligned}
\zeta(\alpha, \theta, t) &= O_1(\alpha, \theta, t) + \sigma_0 O_2(\alpha, \theta, t) \\
\xi(\beta, \theta, t) &= B(\beta)O_3(\beta, \theta, t) \\
&\quad + a \cdot \{O_2(\beta, \theta, t) + \sigma_0 O_3(\beta, \theta, t)\} \\
\eta_1(\alpha, \theta, t) &= C(\alpha)O_2(\alpha, \theta, t) \\
\eta_2(\beta, \theta, t) &= O_2(\beta, \theta, t) \\
&\quad + (A(\beta) + a \cdot C(\beta))O_3(\beta, \theta, t)
\end{aligned}$$

and the series of $O_l(s, \theta, t)$ with $l = 1, 2, 3$ are given by

$$\begin{aligned}
O_l(s, \theta, t) &= 2\pi \sum_{n=0}^{\infty} \Lambda_n(s) T_{n-1+l}(\theta, t) \\
T_0 &= \frac{1 - \cos^2 \theta}{2}, \quad T_1 = t(1 - \cos \theta), \\
T_2 &= \frac{t^2}{2!} \log\left(\frac{1}{\cos \theta}\right), \quad T_3 = \frac{t^3}{3!} \left(\frac{1}{\cos \theta} - 1\right), \\
\cdots \quad T_n &= \frac{t^n}{n!} \frac{1}{n-2} \left(\frac{1}{\cos^{n-2} \theta} - 1\right) \quad \cdots \\
\Lambda_0 &= \frac{\lambda_1 - \lambda_2}{\lambda_1 - \lambda_2}, \quad \cdots, \quad \Lambda_n = \frac{\lambda_1^{n+1} - \lambda_2^{n+1}}{\lambda_1 - \lambda_2} + \Lambda_{n-1} \frac{-1}{L}, \quad \cdots
\end{aligned}$$

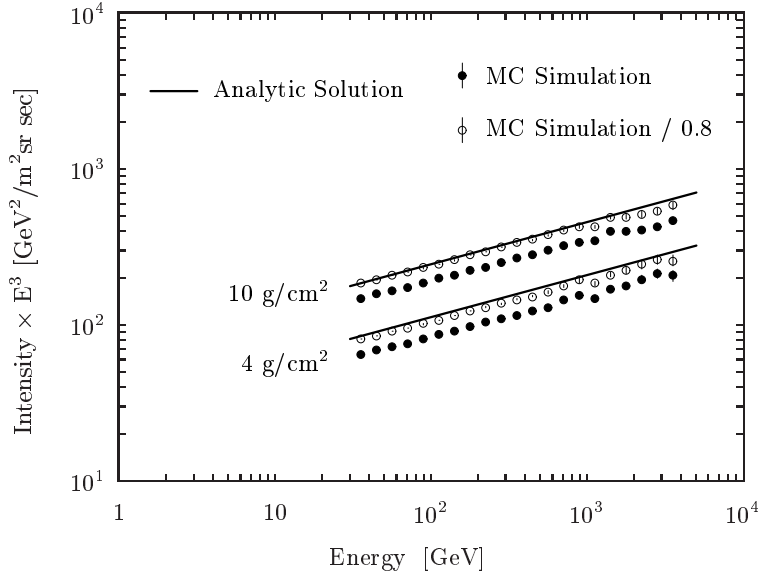


Figure 1: Atmospheric gamma-ray spectra $J_g(E)$ of eq. (8) are compared with the MC results. The solution at 4 g/cm² is equal to eq. (1) multiplied by E^3 . The MC data divided by 0.8 are also shown and good agreement with the analytic solution.

3. Results and Discussions

The analytic solutions obtained here are compared with the results of Monte Carlo simulation(MC). We use the COSMOS simulation code [8] in which the Dpmjet3 [9] is adopted as the hadronic interaction model and the BESS-TeV [10][11] and RUNJOB [12] data for the input proton, helium and CNO spectrum at the top of atmosphere. We have confirmed the consistency of both methods for the cross section using the fundamental processes as shown in Appendix A. In addition, we consider atmospheric electrons directly originating from K and π^\pm mesons, which mainly contribute below 100GeV. The decay modes of $\pi^\pm \rightarrow \mu^\pm \nu(\bar{\nu}) \rightarrow e^\pm \nu \bar{\nu}$, $K_L^0 \rightarrow \pi^\pm e^\mp \nu$, $K^\pm \rightarrow \pi^0 e^\pm \nu$ and so on, are calculated using the recent accelerator data [13], and those contributions are treated as the ratio to electrons produced by gamma rays.

3.1. Atmospheric Electron and Gamma-ray Spectrum

The analytic solution of atmospheric gamma-ray spectrum given by

$$J_g(E, t) = \gamma_{ex}(E, t) \eta_2(t) \quad (10)$$

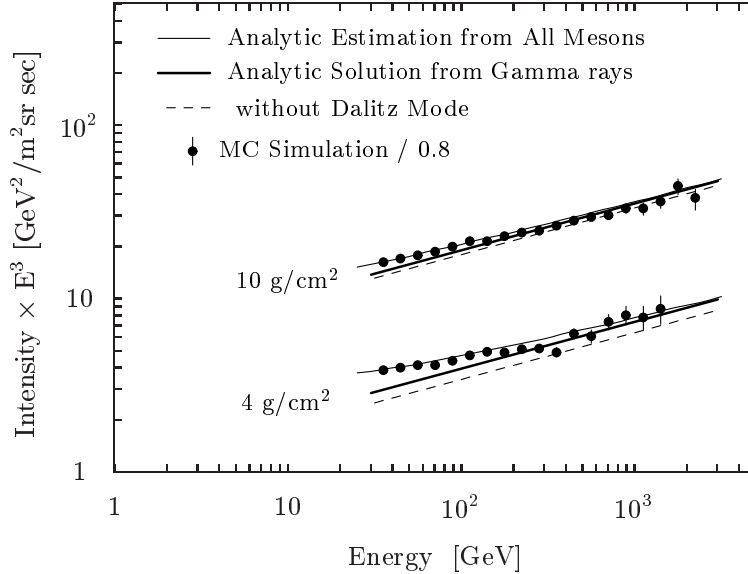


Figure 2: Atmospheric electron spectra are shown at the depth 4, 10 g/cm². The analytic estimation from all mesons (eq. (11)) and the analytic solution $\xi(t)\gamma_{ex}(E, t)$ estimated from gamma-ray spectrum with and without Dalitz decay mode are shown with MC results divided by 0.80.

in eq. (8) and is shown in Figure 1 with the MC results at the depth of 4, 10 g/cm². Figure 1 shows that the gamma-ray spectrum of MC is 20% lower than the analytic solution, which has been indicated in our previous paper [6]: the proton spectrum deconvolved from our observed gamma-ray spectrum assuming the nuclear interaction model of Dpmjet3 is 20% higher than observed primary proton data. Thus the discrepancy of gamma-ray flux in this paper is consistent with the difference between deconvolved and observed proton flux as described in the previous paper [6].

The analytic estimation of atmospheric electron spectrum at the depth t is given by

$$j_{sec}(E, t) = (1 + C)\xi(t)\gamma_{ex}(E, t) \quad (11)$$

as shown in eq. (7). The fraction C represents the contribution from direct productions from K and π^\pm mesons and is shown as the increase of the thin line(all contributions) to the thick line(from gamma rays) in Figure 3. In the fraction C , the K_L^0 mode are mostly dominant as indicated by Orth & Buffington [4]. The contribution from K mesons estimated from the recent

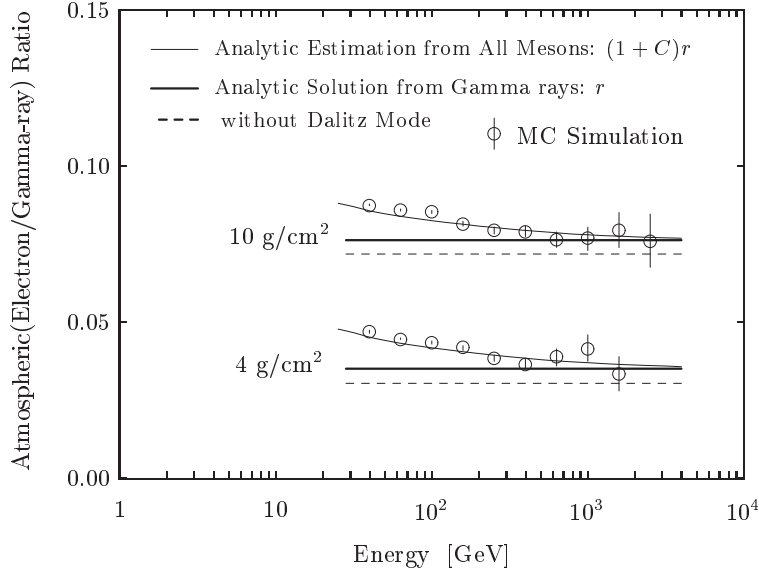


Figure 3: The ratio of atmospheric electrons to gamma-rays. The analytic estimation from all mesons and the analytic solution from gamma-ray spectrum with and without Dalitz mode are compared with Monte Carlo simulation. The ratio r represents $\xi(t)/\eta_2(t)$ and the fraction C represents the contribution from direct productions from K and π^\pm mesons.

accelerator data of K/π ratio [13] is a factor of two smaller than their result.

The atmospheric electron intensity is approximately proportional to t^2 . The comparison with MC is shown in Figure 2, in which the spectrum of MC is divided by 0.80 to correct the discrepancy of gamma-ray spectrum. In the energy range above several hundred GeV, we notice that the Dalitz decay mode contributes more than 10 % to the ratio at high altitude above 4 g/cm^2 , and the estimated spectrum is in good agreement with the corrected MC simulation in all energy range. The atmospheric electrons become a larger fraction of the observed electrons in the higher energy region because of the harder spectrum than the primary electron one.

We investigate the consistency between the analytic estimation and MC by comparing the ratio of atmospheric electrons to gamma rays, which is able to exclude the discrepancy of gamma ray spectrum. The ratios compared at the depth $t = 4, 10 \text{ g/cm}^2$ are shown in Figure 3, which shows good agreement between the analytic estimation and MC simulation. The Dalitz contribution has a constant value and does not vary with the depth t , since

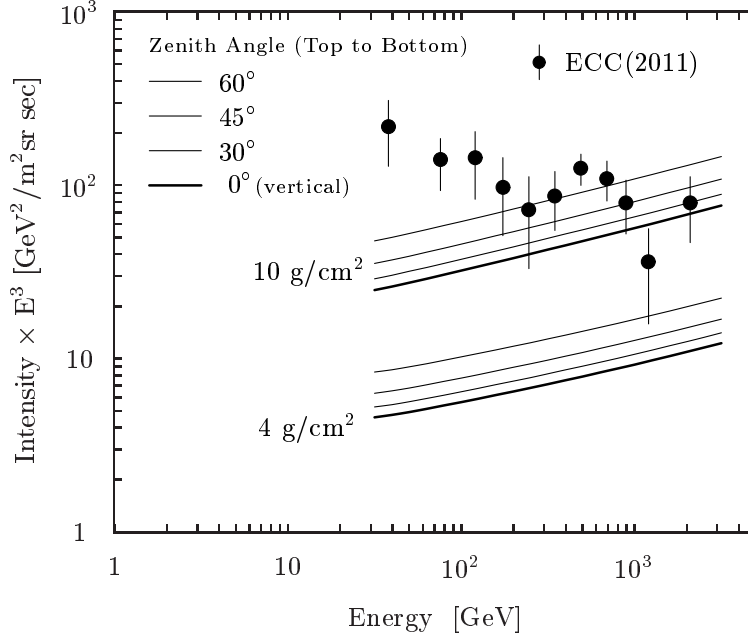


Figure 4: The correction term of atmospheric electrons of eq. (13) with acceptance angle of 30° , 45° , 60° and vertical for detectors at 4 , 10 g/cm^2 , and compared with the result of primary electron spectrum.

Dalitz electrons approximately increase in proportional to gamma rays and t , while electrons produced by gamma rays are proportional to t^2 . It means that the Dalitz mode plays a more important role at the higher altitude above several hundreds GeV. On the other hand, below 100 GeV the direct productions from K and π^\pm mesons become larger than that from the Dalitz mode.

3.2. Observation and Correction

The primary electron spectrum is obtained from

$$\pi(E, 0) = \frac{j_{ob}(E, \theta, t)}{\zeta(\alpha, \theta, t)} - \gamma_{ex}(E, t) \frac{\xi(\beta, \theta, t)}{\zeta(\alpha, \theta, t)} \quad (\text{m}^2 \cdot \text{sr} \cdot \text{sec} \cdot \text{GeV})^{-1}, \quad (12)$$

using the eq. (9), in which $1/\zeta$ is the correction term of the energy reduction by bremsstrahlung. The second term is the correction term of atmospheric electrons which are observed at the depth t within zenith angle θ and corrected by energy reduction to the top of the atmosphere. The term ξ/ζ is

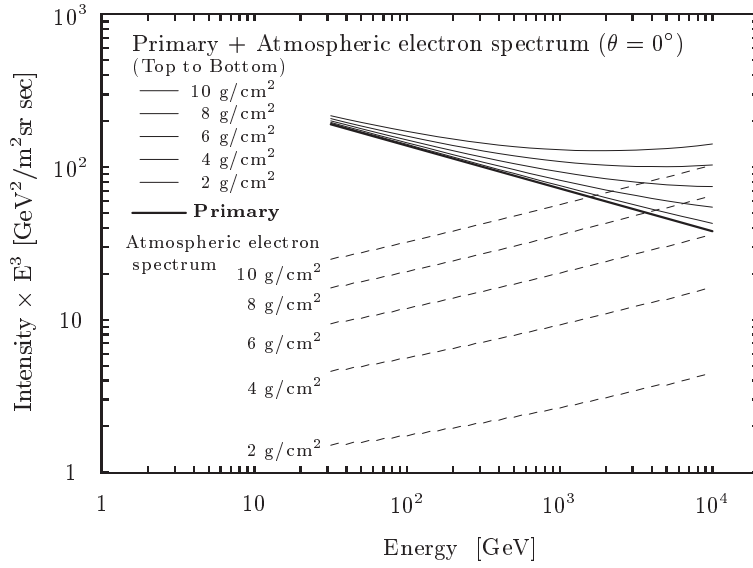


Figure 5: The primary plus atmospheric electron spectrum (thin line) at each depth above 10 g/cm² including the extrapolation above 3 TeV. The primary electron spectrum (thick line) with the simple power law is estimated from the recent result below 3 TeV [3]. The atmospheric electron spectra (dashed line) are given by eq. (13).

approximately proportional to t^2 . The eq. (12) indicates that all the observed electrons are firstly corrected by bremsstrahlung loss energy, and then, the atmospheric electrons are statistically subtracted.

Finally the atmospheric electron spectrum corrected at the top of the atmosphere is given by

$$J_{sec}(E, t) = (1 + C)\gamma_{ex}(E, t) \frac{\xi(\beta, \theta, t)}{\zeta(\alpha, \theta, t)} (\text{m}^2 \cdot \text{sr} \cdot \text{sec} \cdot \text{GeV})^{-1} . \quad (13)$$

Figure 4 indicates the correction term of atmospheric electron spectra of eq. (13) for the different acceptance angle of each detector at 4, 10 g/cm², compared with the primary electron spectral data. The fraction C practically has no influence on the correction of the primary electron spectrum. Further in Figure 5, we show the primary electron spectrum, the atmospheric electron spectra of eq. (13) and total spectra at each depth above 10 g/cm². It is shown that the balloon experiment for electrons above 1 TeV requires the observation at a high altitude, since correction terms dominate the data at 10 g/cm².

4. Conclusions

In the balloon observations of cosmic-ray electrons, the atmospheric electrons are inevitably included in the observed spectrum and necessary to be subtracted to obtain the primary electron spectrum. The atmospheric electrons are mostly produced by the atmospheric gamma-ray conversion, and above several hundred GeV, around 10% of them at the depth of 4 g/cm² are produced by the Dalitz decay mode. We have treated these processes analytically and obtained accurate solutions. The result shows that the atmospheric electron spectrum obtained by MC is 20% lower than that of the analytic estimation. The discrepancy comes from the difference of atmospheric gamma-ray spectrum, since the ratio of atmospheric electrons to gamma rays shows a good agreement. The difference of the gamma-ray spectrum comes from the uncertainties of the primary cosmic-ray hadron spectra and the nuclear interaction models used in the MC calculations, together with the statistical error of 10 % included in the observed gamma-ray spectrum of eq. (1). The Dalitz mode gives a constant contribution to the atmospheric electron/gamma-ray ratio and becomes particularly important at the higher altitude above 4 g/cm². On the other hand, in the lower energy range below 100 GeV the direct contributions of electrons from K and π^\pm mesons

become larger than the Dalitz contribution, although atmospheric electrons below 100 GeV have almost no influence on the correction of the primary electron spectrum.

The astrophysical significance to search for the cosmic ray sources by primary electrons become more important at higher energy regions, however, the contribution of the background atmospheric electrons increases seriously in the balloon observations in TeV region. Thus the observation of TeV electrons requires the higher altitude, and more precise estimates of the atmospheric electrons are required than that of several hundred GeV region. Although these conditions are getting more difficult at higher energy region, the experiments in TeV region are the most important to search for cosmic-ray sources [2].

5. Acknowledgment

We sincerely thank Prof. J. Arafune for his helpful discussions on the contribution of the Dalitz pair to the atmospheric electrons. We also thank Dr. M. Honda for his valuable comments on the nuclear interaction data. We are grateful to Prof. R. J. Wilkes for his careful reading and useful comments of the manuscript.

References

- [1] J. Nishimura, M. Fujii et al., *Astrophys. J.*, 238 (1980) 394-409
- [2] T. Kobayashi, Y. Komori, K Yoshida and J Nishimura *Astrophys. J.*, 601 (2004), 340-351
- [3] T. Kobayashi, Y. Komori, K Yoshida, J Nishimura et al., submitted to *Astrophys. J.*
- [4] C.D. Orth and A. Buffington, *Astrophys. J.*, 206 (1976) 312-332
- [5] J. Nishimura, *Handbuch der Physik*, 46, II, 1, Springer, 1967
- [6] K Yoshida, R Ohmori, T. Kobayashi, Y. Komori, Y. Sato and J. Nishimura, *Phys. Rev. D* 74, 083511 (2006) 1-13
- [7] K. Nakamura et al.(Particle Data Group) *J.Phys.*, G37 (2010) 075021

- [8] K. Kasahara <http://cosmos.n.kanagawa-u.ac.jp/>
- [9] S. Roesler et al., Report No. SLCA-PUB-8740, Proc. of Monte Carlo 2000, 72 (2000) 23
- [10] T. Sanuki, M. Motoki et al., *Astrophys. J.*, 545 (2000) 1135-1142
- [11] S. Haino, T. Sanuki et al., *Phys. Lett. B*, 594 (2004) 35-46
- [12] A.V. Apanasenko, et al., *Astropart. Phys.*, 16 (2001) 13-46
- [13] The ALICE Collaboration, *Eur. Phys. J. C*, 71, 6, 1655 (2011) 1-22

Appendix A. Fundamental Parameters

We calculate the fundamental process and compare the result with that of MC to confirm the consistency of cross section. When gamma rays or electrons pass through the thickness t of the air, the number of electrons $\pi(E, t)dE$ and gamma rays $\gamma(E, t)dE$ with energies between E and $E + dE$ satisfy the transport equations as:

$$\begin{aligned}\frac{\partial\pi(E, t)}{\partial t} &= -A'\pi(E, t) + B'\gamma(E, t) \\ \frac{\partial\gamma(E, t)}{\partial t} &= C'\pi(E, t) - \sigma_0\gamma(E, t)\end{aligned}$$

The physical meaning of each parameter A' , B' , C' and σ_0 is explained in the section 2.1 in this text. The functional forms of the operators A' , B' , C' , σ_0 and $\lambda_{1,2}$ used in the equations are given in several references (e.g. [5]) as

$$\begin{aligned}A(s) &= 1.3603\frac{d}{ds}\ln\Gamma(s+2) - \frac{1}{(s+1)(s+2)} - 0.07513, \\ B(s) &= 2\left(\frac{1}{s+1} - \frac{1.3603}{(s+2)(s+3)}\right), \\ C(s) &= \frac{1}{s+2} + \frac{1.3603}{s(s+1)}, \\ \sigma_0 &= 0.7733, \\ \lambda_{1,2}(s) &= \frac{1}{2}\left[-(A(s) + \sigma_0) \pm \{(A(s) + \sigma_0)^2 - 4(A(s)\sigma_0 - B(s)C(s))\}^{\frac{1}{2}}\right],\end{aligned}$$

where $s+1$ corresponds to a power-law index of the solutions. The numerical values of $A(s)$, $B(s)$ and $C(s)$ used in this paper are listed as

$$\begin{aligned}A(2.30) &= 1.6743, \quad B(2.30) = 0.4867, \quad C(2.30) = 0.4118, \\ A(1.73) &= 1.4270, \quad B(1.73) = 0.5784, \quad C(1.73) = 0.5561.\end{aligned}$$

We calculate the gamma ray conversion process and confirm the agreement between analytical method and MC. If the initial condition is given by

$$\begin{aligned}\pi(E, 0) &= 0, \\ \gamma(E, 0) &= k_g\left(\frac{E}{100 \text{ GeV}}\right)^{-\beta-1}\end{aligned}$$

Table A.1: The number of Electrons produced by gamma rays at 100 GeV, which is divided by the initial number of k_g .

Depth (t)	0.4 g/cm ²	4.0 g/cm ²
Analytic Solution	6.229×10^{-3}	5.596×10^{-2}
MC	$(6.25 \pm 0.04) \times 10^{-3}$	$(5.61 \pm 0.04) \times 10^{-2}$

with $\beta = 1.73$, the solution of produced electron and gamma ray spectrum at the depth t becomes

$$\begin{aligned}\pi(E, t) &= \frac{\gamma(E, 0)}{\lambda_1 - \lambda_2} B(\beta) [e^{\lambda_1 t} - e^{\lambda_2 t}], \\ \gamma(E, t) &= \frac{\gamma(E, 0)}{\lambda_1 - \lambda_2} [A(\beta)(e^{\lambda_1 t} - e^{\lambda_2 t}) \\ &\quad + \lambda_1 e^{\lambda_1 t} - \lambda_2 e^{\lambda_2 t}].\end{aligned}$$

In Table A.1, the number of electrons $\pi(E, t)$ produced by gamma ray conversion are shown at the depths of 0.4 g/cm² and 4.0 g/cm² and compared with the results of MC. These values directly represent the cross section of pair production and one can find that the cross section agrees with each other within ± 0.5 %.

Appendix B. Dalitz electron contribution

We include the contribution of Dalitz electrons represented by a fraction of gamma-ray production rate (eq (5)). The coefficient a is estimated from the sum of Dalitz electrons of π^0 , η and K^0 decays.

In the π^0 decay, the branching ratio of the first mode is given by $B_m \equiv B(\pi^0 \rightarrow \gamma\gamma) = (98.798 \pm 0.032)\%$ and that of the second mode is $B_D \equiv B(\pi^0 \rightarrow e^+e^-\gamma) = (1.198 \pm 0.033)\%$ [7]. We require the the ratio of Dalitz electrons to gamma rays from the π^0 meson spectrum $\propto E^{-\beta-1}$ ($\beta = 1.73$), and it becomes $B_D/(2B_m)/(2/(\beta+1)) = 4.4 \times 10^{-3}$, if the distribution of pair electrons is uniform. Precise estimate gives a somewhat different distribution of the pair production with two peaks, so that the value is slightly corrected and becomes 4.6×10^{-3} .

The ratio of Dalitz electrons to gamma rays for each decay is listed in Table B.2. The major contribution of Dalitz electrons comes from π^0 decay. The η decay gives the small contribution, and the K^0 decay can be neglected.

Table B.2: Dalitz contributions of π^0 , η and K^0 decays

	π^0	η	K^0
Gamma-ray ($\gamma\gamma$) mode	98.8 %	39.3 %	98.8 %
Dalitz ($e^+e^-\gamma$) mode	1.2 %	0.68 %	1.2 %
Dalitz electron / γ -ray (r)	4.6×10^{-3}	6.6×10^{-3}	4.6×10^{-3}
Fraction of γ -ray production (p)	1/1.19	0.16/1.19	0.03/1.19
Ratio in upper atmos. ($= r \times p$)	3.9×10^{-3}	0.9×10^{-3}	0.1×10^{-3}

The net fraction of Dalitz decay electrons to the observed gamma rays are given by 4.9×10^{-3} .